# Diffusion and condensation of lithium atoms in single-walled carbon nanotubes

Mingwen Zhao,* Yueyuan Xia, and Liangmo Mei
*Department of Physics, Shandong University, Jinan 250100, China*
(Received 11 July 2004; revised manuscript received 15 November 2004; published 12 April 2005)

We have carried out theoretical investigations to explore the diffusion of lithium on the exteriors and the interiors of single-walled carbon nanotubes (SWNTs). We found that lithium can adsorb on both interior and exterior surfaces with adsorption energy around −2.44 eV. Lithium has a higher mobility with the diffusion barriers less than 0.2 eV on both the exteriors and interiors of SWNTs. The diffusion barriers (exo- and endohedral) of lithium depend on the radius and chirality of SWNTs. The lithium capacity trapped inside SWNTs increases with the increasing tube diameter and can be as high as $LiC_{2.6}$ in a (10,10) SWNT. These lithium atoms tend to form single- or multishelled coaxis nanotubes, together with a linear atomic chain in the axis at low temperature depending on the diameter of SWNTs, suggesting a potential way to synthesize small metal nanotubes and metal nanowires.

DOI: 10.1103/PhysRevB.71.165413 PACS number(s): 61.48.+c, 71.15.Mb, 71.15.Pd, 71.20.Tx

## INTRODUCTION

Carbon nanotubes are attracting more interest as molecular containers with applications as hydrogen fuel cells[1] and lithium batteries,[2] due to their unique structure and properties. Single-walled carbon nanotubes (SWNTs) can be thought to arise from the folding of a graphite sheet. The nanotubes typically aggregate into bundles termed nanoropes, which consist of SWNTs held together by van der Waals forces, forming close-packed two-dimensional triangular lattices.[3] The interstitial channels between the tubes and the interiors of the nanotube themselves are ideal containers for intercalation of foreign molecules and atoms, such as $H_2$,[1,4] He,[4] $C_{60}$,[5] and Li.[6,7] For example, hydrogen molecules can be physically adsorbed on the exterior surface of SWNTs[1] or trapped in the interiors of tubes provided that a hydrogen atom can enter into the tube through open ends or tube wall.[8,9]

For the interiors of SWNTs, the motion of $H_2$ is not diffusion limited because the interactions between $H_2$ and SWNTs are mainly dominated by van der Waals forces, and ultimately result in configurations with linear lines or coaxis cylindrical shells.[8–11] Interestingly, the van der Waals surface forces hydrogen to form quasi-one-dimensional lattices with the hydrogen molecular orientation highly polarizing along the axial direction of the tube at low temperature.[12] In addition, one-dimensional carbon structures formed inside carbon nanotubes through self-assembling of $C_{60}$ and carbon atoms have also been revealed experimentally.[5,13]

Li-nanotube complexes, which are of technological importance as anodes of Li-ion batteries, have been synthesized by intercalating lithium atoms both into the interstitial channels between carbon nanotubes and into the interiors of the nanotubes themselves. The energy density of Li-ion batteries largely depends on the host materials of the anode. Graphitic carbon anodes are used instead of metallic Li electrodes in most batteries because of both safety and cycle efficiency concerns,[14] although this substantially reduces the energy density of the battery as compared to metallic Li. Graphite, intercalated with Li, can improve the energy density of Li-ion batteries. Performance can be significantly enhanced if one could somehow boost the Li/C ratio inside the host materials. The limit for graphite intercalation under ambient conditions is one lithium atom per six carbons ($LiC_6$). However, higher lithium capacity up to $Li_{1.6}C_6$ and $Li_{2.7}C_6$ has been achieved in SWNTs,[6] and is predicted with enhanced anode stoichiometry $LiC_2$.[15]

Another key to superior battery performance using nanotubes lies in the ability of Li ions to enter and leave the nanotube interiors at a reasonable rate. The motion of lithium inside SWNTs has been studied using first-principles calculations, and it has been predicted that lithium ions can enter into SWNTs through topological defects and open-ended nanotubes.[15–17] The diffusion barriers for Li motion in the interstitial channels between the nanotubes and inside the nanotubes themselves turn out to be very low for some selected nanotubes. However, some relevant issues are not clearly understood, such as: (1) Do the diffusion barriers of lithium inside and outside SWNTs depend on the diameter and chirality of the tubes? (2) What is the morphology of lithium atoms trapped inside SWNTs, especially for the tube of large diameter? (3) Can lithium atoms form quasi-one-dimensional lattices at low temperature similar to the case for $H_2$? (4) What is the capacity of Li trapped inside SWNTs of different diameters? To address these issues, the studies of dynamics of Li relevant to the diffusion and condensation processes inside/outside SWNTs of different diameters and chiralities are highly desirable.

## THEORETICAL APPROACH AND COMPUTATION

Atomistic simulations of Li-SWNT complexes were preformed using an efficient first-principles program known as FIREBALL.[18] This code is based on density-functional theory (DFT) adopting a localized linear combination of numerical atomic-orbital basis for the description of valance electrons and norm-conserving separable pseudopotentials for the atomic core. The basis functions used are a set of slightly excited pseudoatomic wave functions computed within DFT. These FIREBALL wave functions are chosen such that they vanish at some radius $r_c$. The pseudopotentials were con-

 

structed using the scheme of Fuchs and Scheffler[19] to describe the valance electron interaction with the atomic core, and expressed in the form of Hamann.[20]

A single numerical (SN) basis set $sp^3$ was employed for carbon and lithium atoms throughout the calculations. The localized pesudoatomic orbitals were constructed with a confinement radius of 7.10 $a_B$ for the 2*s* state of lithium, while the 2*s* and 2*p* orbitals of carbon were confined in a sphere with radius of 4.00 $a_B$ and 4.40 $a_B$, respectively. The model of electronic exchange-correlation functional employed in these calculations was a generalized gradient approximation (GGA) of the form containing Becke exchange (B88) with Lee-Yang-Parr (LYP) correlation.[21,22] This scheme has been successfully used to study nanosystems involving SWNTs in previous literatures.[23–25] To test its validity in describing Li-Li interaction, we calculated bulk lithium in the bcc phase using the periodical boundary condition. The equilibrium lattice constant was found to be 3.49 Å, in good agreement with the experimental result 3.50 Å,[26] while the cohesive energy was 1.33 eV/atom, a bit lower than 1.84 eV/atom from other DFT calculations.[27] For small Li-C clusters, such as $LiC_6$, our calculation gave the results comparable to those from the high level DFT calculations (B3LYP/6-311++$G^*$) within GAUSSIAN 98[28] with bond lengths and binding energies differences less than 10%.

When studying the diffusion of Li ions, the periodical boundary condition along the tube axis was used for the SWNTs. The supercells selected for armchair SWNTs contain ten layers of carbon atoms, while eight layers of carbon atoms are included for zigzag SWNTs. In order to determine the energetically most economical diffusion pathways for the Li ions, we push the ion over the surface with a small, constant force, while monitoring the total energy. Since the ion is constrained in one direction only, it is free to move in the directions perpendicular to the applied force, thereby enabling the ion to find its optimum path. All other atoms are relaxed continuously in response to the Li ion motion. A similar method has been found as a viable and realistic alternative to a costly point-by-point determination of the potential energy surface.[17,29]

## RESULTS AND DISCUSSION

The interaction between lithium and SWNTs is a well-known cation-$\pi$ interaction that has been studied thoroughly by high-level *ab initio* calculations[30,31] and by experiment.[32] In the Li-benzene system, the most favorable site of lithium is over the center of a hexagon. The energy associated with moving lithium toward the center of a hexagon of a (5,5) SWNT on the interior and exterior of the tube along a direction perpendicular to the hexagon is shown in Fig. 1. The total energy corresponding to the configuration of a lithium trapped in the center of the (5,5) SWNT is the zero energy. All carbon atoms were relaxed for each calculation point as Li was brought closer to the SWNT surface. Two local minima located inside/outside of the tube in this figure clearly indicate that lithium can adsorb on both the inside and outside surfaces of the tube. The corresponding equilibrium configurations are presented in the insets of the figure.

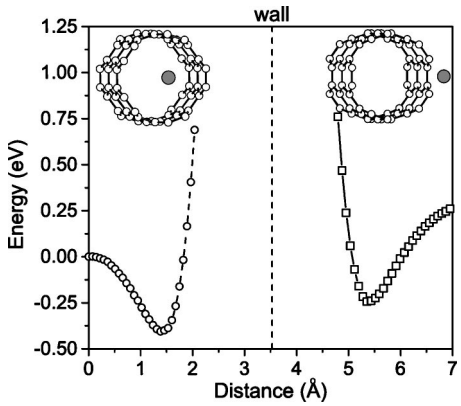


FIG. 1. The relative energy of a (5,5) SWNT with an adsorbed lithium varies as the endo- and exohedral approaches of the lithium toward the center of a carbon hexagon in the tube wall. The horizontal axis is the distance of the lithium to the tube axis. The structure was relaxed during the approaches. The equilibrium configurations of endo- and exohedral adsorption of a lithium on the tube wall are shown as the insets of this figure, where the black balls and white circles denote lithium and carbon atoms, respectively.

The equilibrium distance between lithium and the center of the hexagon are 2.06 and 1.87 Å for endo- and exohedral adsorption, respectively, and both are close to the result of a Li-benzene compound at the B3LYP/6-31$G^*$ level, 1.88 Å.[16]

The structural distortion caused by the adsorption of the lithium was found to be very slight. The binding energies between the lithium and (5,5) SWNT are calculated to be −2.33 and −2.17 eV for endo- and exohedral adsorption, respectively.[33] These results are lower than those of the Li-benzene compound where calculations give −1.84 eV at the B3LYP/6-31$G^*$ level and −1.67 eV at the highest level B3LYP/6-311++$G^*$.[16] This is mainly due to the curvature-induced effects in SWNTs and the simple base sets (SN) used in our calculations. However, the energy difference between endo- and exohedral adsorptions obtained from our calculation, 0.16 eV, is in good agreement with the result of 0.20 eV from another *ab initio* calculation.[15] Mulliken population analysis also shows that the lithium is almost completely ionized, indicating that the interaction between the lithium and SWNTs is likely ionic, which is consistent with other results.[15,17] Moreover, the difference in binding energy between lithium located at the center and the tube edge is found to be −2.0 eV. The difference is probably due to the ionization of SWNTs to lithium atoms and suggests that SWNTs actually act as an attractor for the lithium ion. Similar results also hold for the Li ions entering the interstitial channel in carbon nanoropes.

Considering the importance of lithium mobility in improving the performance of Li batteries, we investigated the diffusion barriers of lithium as it moves from neighboring sites. Both interior (endo-) and exterior (exo-) surfaces were considered for some selected SWNTs with different diameters and chiralities, (5,5), (6,6), (8,8), (10,10), (9,0), and (12,0). The energy variations along different pathways over/below the walls of (5,5), (10,10), and (9,0) SWNTs are shown in Figs. 2(a)–2(c). Figure 3 gives the variations of

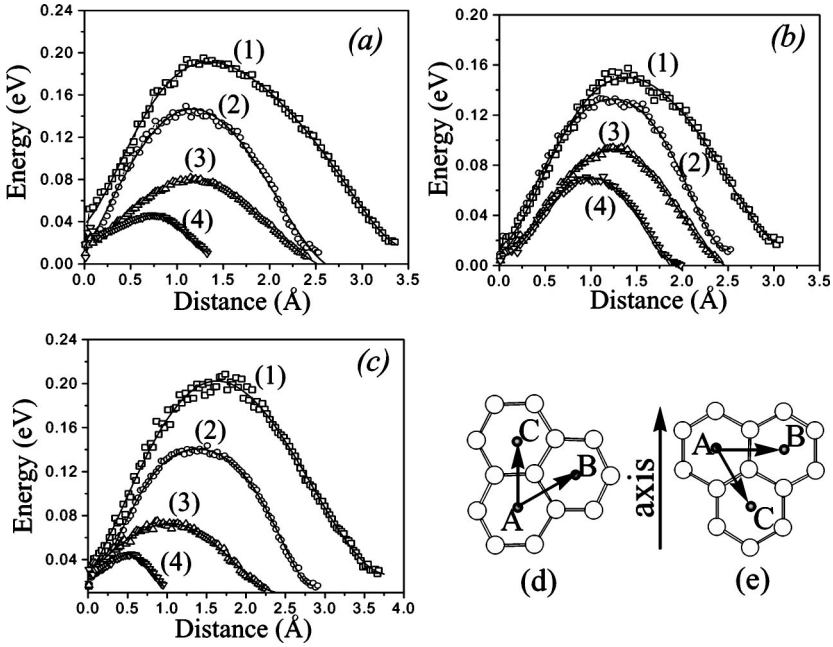


FIG. 2. Variation of the total energies of (a) (5,5), (b) (9,0), and (c) (10,10) SWNTs with a lithium adsorbed on the interior (endo-) and exterior (exo-) surface as the lithium is diffusing from one stable adsorption site to the adjacent adsorption sites along different paths shown as (d) and (e): (1) A→B (exo); (2) A→C (exo); (3) A→C (endo); and (4) A→B (endo). For each path, the total energy of the initial structure is set to zero. The solid lines are the fitting results.

diffusion barriers along different pathways as a function of tube diameter, while the corresponding values are listed in Table I. We can see two obvious features from these results.

First, the energetically most economical diffusion paths of Li inside and outside SWNTs are quite different, and depend on the chirality of the tubes as well. For a (5,5) SWNT as an example, the most economical pathway of endohedral diffusion is in the direction from A to B, while the exohedral pathway is from A to C [Fig. 2(d)]. However, for a (9,0) SWNT, the most energetic pathway for endohedral diffusion is around the tube axis [from A to B, see Fig. 2(e)], while that of exohedral diffusion is helical around the tube axis [from A to C, see Fig. 2(e)]. This is related to the potential profiles along different directions on the curved hexagonal layers. The maximum energy of the Li-SWNT system as a single lithium atom moving along these pathways corresponds to the configuration where the lithium is straight above (below) a C—C bond for exo- (endo-) hedral diffusion. On a flat graphite layer, these maximum energies are equal because of structural symmetry. For the case of SWNTs, however, the asymmetry caused by curvature effect separates these maximum energies, giving rise to different diffusion barriers. The chiral dependence of the economical pathway may characterize the diffusion behavior of lithium inside/outside SWNTs. The trajectory of lithium diffusion inside armchair SWNTs, for instance, may be helical around the tube axis, whereas for exohedral diffusion, the trajectory may likely be along the tube axis.

Second, the diffusion barrier slightly depends on the tube diameter. With increasing tube diameter, the endohedral diffusion barrier increases, whereas the exohedral barrier decreases (Fig. 3). The diffusion barrier of lithium inside a (5,5) SWNT is about 0.046 eV from our calculation, in good agreement with 0.035 eV of another *ab initio* investigation.[17] For a (10,10) SWNT, the endohedral diffusion barrier increases to 0.070 eV. The exohedral diffusion barrier is 0.147 eV for a (5,5) SWNT, and slightly decreases to 0.133 eV for a (10,10) SWNT. We should mention here that the diffusion barrier of Li in the exterior of a (5,5) SWNT obtained from our calculation is much higher than that of lithium in the interstitial channel in nanorope (0.045 eV) obtained from another *ab initio* investigation.[17] The reason is that we only investigated an isolated SWNT and did not take the contribution of interactions between adjacent tubes in the nanorope into account. Moreover, due to the weakening of the curvature effect with increasing tube diameter, the difference in diffusion barriers along different pathways decreases (Fig. 3). The largest difference between exo- and endohedral diffusion barriers decreases from 0.149 eV for a (5,5) SWNT to 0.080 eV for a (10,10) SWNT. It can be expected that these diffusion barriers will saturate at the same value corresponding to the diffusion barrier of a lithium on graphene as the tube diameter is large enough.

Because lithium atoms are ionized and have high mobility inside SWNTs, they will rearrange themselves to minimize the electrostatic repulsion when placed randomly. We randomly placed lithium atoms inside different open-ended SWNTs, then annealed the Li-SWNT systems at 1000 K for

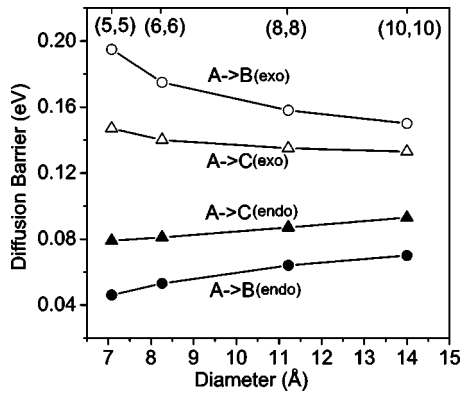


FIG. 3. The variation of diffusion barrier along different pathways as a function of tube diameter.

TABLE I. The diffusion barriers (eV) of a single lithium on the inside (endo) and outside (exo) surface of isolated SWNTs of different sizes and chiralities along the pathways shown in Figs. 2(d) and 2(e).

| | (5,5) | (6,6) | (8,8) | (10,10) | (9,0) | (12,0) |
|---|---|---|---|---|---|---|
| A→B (exo) | 0.195 | 0.175 | 0.158 | 0.150 | 0.202 | 0.183 |
| A→C (exo) | 0.147 | 0.140 | 0.135 | 0.133 | 0.140 | 0.134 |
| A→C (endo) | 0.079 | 0.081 | 0.087 | 0.093 | 0.073 | 0.075 |
| A→B (endo) | 0.046 | 0.053 | 0.064 | 0.070 | 0.045 | 0.057 |

2 ps and subsequently cooled down to 300 K for 1 ps. In order to determine the structure of lithium trapped inside SWNTs, we further relaxed the Li-SWNT systems at 100 K for about 2 ps. We did not use periodical boundary conditions along the tube axis for these SWNTs. The atoms in the tube tips are free to move, enabling lithium to get away from and enter into SWNTs throughout simulations. Equilibrium states of lithium atoms trapped inside SWNTs can therefore be obtained after long-time simulations. We found that the lithium atoms formed a linear chain along the tube axis inside a (6,0) SWNT [as shown in Figs. 4(a) and 4(b)]. The corresponding pair distribution functions in the radial direction, $g(r)$, and in the axial direction, $g(z)$, presented in Figs. 4(a) and 4(b) display the character of a one-dimensional lattice with the average Li-Li bond length of 2.91 Å. Due to the confinement of SWNT and size effect, the bond length in this atomic chain is much shorter than that in bulk materials (3.50 Å in the bcc phase). This configuration is very similar to the one-dimensional carbon nanowire formed inside multiwalled carbon nanotubes.[13] For a (5,5) SWNT, the interior space is large enough for lithium to form a cylindrical surface of radius 1.77 Å [as shown in Fig. 4(c)]. The distance from the Li-cylindrical surface to the wall of the (5,5) SWNT is about 1.83 Å, which is shorter than the equilibrium distance of the single lithium to the wall of the (5,5) SWNT, 2.06 Å. The average bond length between lithium atoms is 2.80 Å. For large-size SWNTs, the trapped lithium atoms tend to form a multishell structure composed of coaxial tubes with a linear chain in the axis depending on the tube radius [as shown in Figs. 4(d)–4(f)]. The equilibrium configuration of lithium atoms trapped inside a (7,7) SWNT is a cylindrical surface of radius 2.64 Å with a linear line in the axis [Fig. 4(d)]. The average distance between adjacent lithium atoms is 2.86 Å. The lithium atoms form a double shell structure with the radii of 1.81 and 4.42 Å inside a (9,9) SWNT [Fig. 4(e)]. For a (10,10) SWNT, the equilibrium configuration of the trapped lithium atoms is composed of two coaxial tubes together with a linear atomic chain in the center [Fig. 4(f)]. The radii of these coaxial lithium tubes are 2.80 and 5.23 Å, respectively. The formation of cylindrical surfaces is related to the axial symmetry of the potential profile of lithium inside SWNTs in response to the tubular structure of SWNTs. The potential profile along/around tube axis inside SWNTs is more flat as compared with that in the radial direction (Fig. 1). This potential surface forces lithium atoms to arrange themselves on a set of coaxis cylindrical surfaces or a linear chain to minimize energy. Obviously, these multishell and linear configurations are quite different from the cubic structure of the corresponding bulk materials.

It is very interesting to find out if these lithium atoms have some structural order along the tube axis. The equilibrium configuration of lithium atoms trapped inside a (7,7) SWNT is shown in Fig. 5(a) (side view). The pair distribution function in the axial direction $g(z)$ of the linear atomic chain in the center (denoted by black circles) clearly displays the character of one-dimensional lattice with the average Li-Li bond length of 2.90 Å. For the lithium tube (denoted by gray circles), although the regularity is not clear from the axial pair distribution function $g(z)$ [Fig. 5(c)], we can still find out some evidence of ordered structure. The lithium atoms tend to form a curved triangular structure [as indicated by the deformed hexagon and rhombus in Fig. 5(a)] in some special local areas. This implies that the lithium tube formed inside SWNTs may be described as rolling up a sheet of the

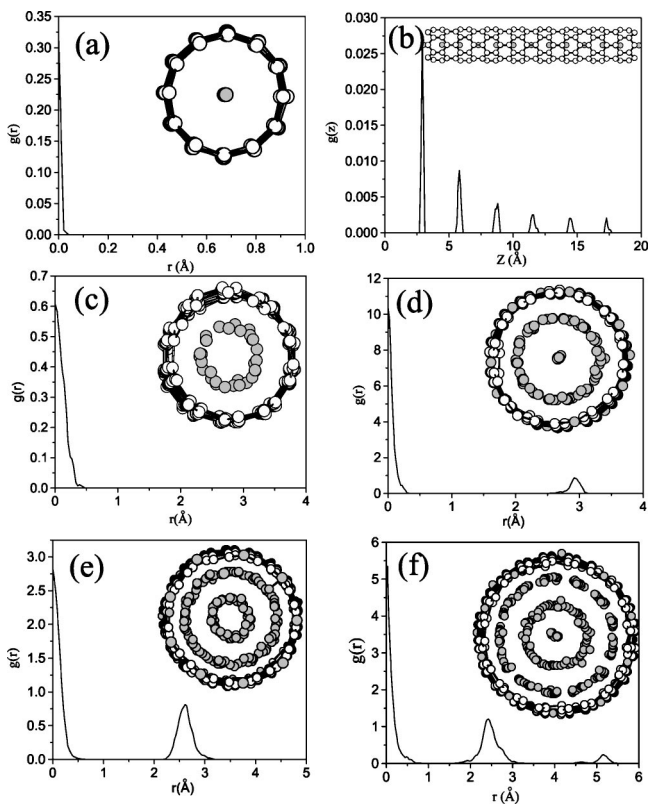


FIG. 4. The pair distribution functions in the radial direction $g(r)$ and axial direction $g(z)$, and the equilibrium configurations of lithium trapped inside (a), (b) (6,0) SWNT, (c) (5,5) SWNT, (d) (7,7) SWNT, (e) (9,9) SWNT, and (f) (10,10) SWNTs. White and gray circles in this figure represent carbon and lithium atoms, respectively.

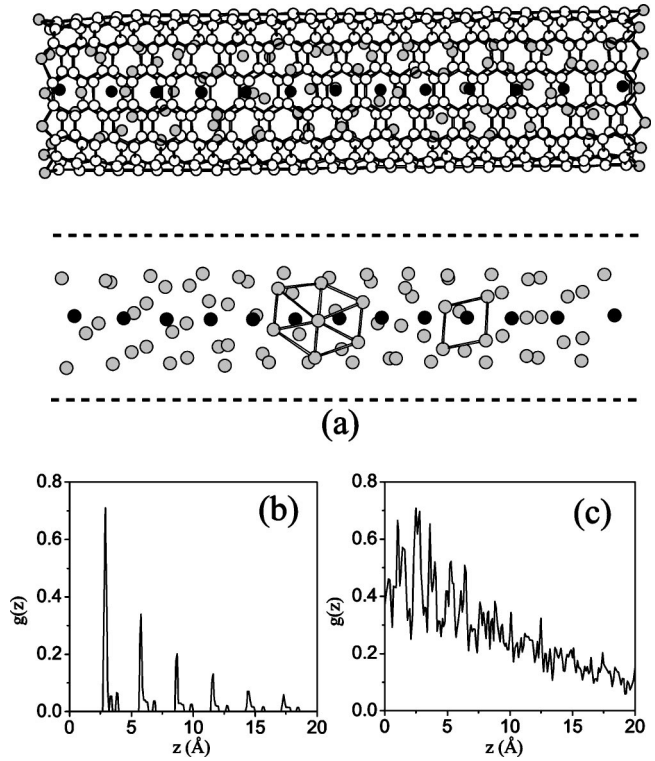


FIG. 5. (a) The equilibrium configuration of lithium trapped inside a (7,7) SWNT (side view). Carbon atoms are denoted by white circles, while lithium atoms are represented by gray and black circles. The dashed lines indicate the wall of a (7,7) SWNT. (b) The pair distribution function in the axial direction $g(z)$ of the linear atomic chain in the center (denoted by black circles). (c) The pair distribution function in the axial direction $g(z)$ of the lithium tube (denoted by gray circles).

triangular network. This structure is very similar to that of suspended gold nanowires made in ultrahigh vacuum.[34] Presently, we cannot obtain the high-ordered tubular configurations of lithium atoms trapped inside SWNTs from molecular dynamic simulations based on DFT calculations because of the very large system sizes involved and the time-scale problem. However, it is believable that such ordered structures of lithium trapped inside SWNTs exist especially at low temperature because of the flat potential profile along/around the tube axis as revealed in our calculations. In view of the high possibility of lithium entering into SWNTs either through topological defects in the sidewall or through a soakage effect of the SWNT to lithium from the opened ends, it is feasible to obtain quasi-one-dimensional triangular lattices of lithium trapped inside SWNTs at low temperature. Gold nanowires with similar morphology have been synthesized by an electron beam thinning technique.[35] Our calculations provide a promising alternate way to synthesize small metallic nanotubes and nanowires. These structures, if synthesized, may be important in connection with quantum devices,

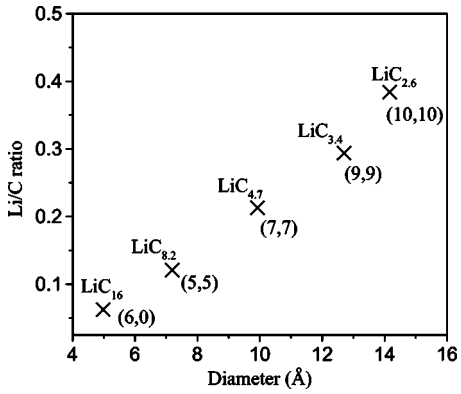


FIG. 6. The variation of Li/C ratio as a function of the diameter of SWNTs.

due to the quantum transport of the conduction electrons in these structures and the coupling between the metallic nanowires and SWNTs.

We also evaluated the lithium capacity inside different SWNTs on the base of the equilibrium configurations described above. The Li/C ratios corresponding to SWNTs with different diameters are plotted in Fig. 6. We found the lithium capacity inside the SWNT is approximately proportional to the diameter of the tubes. The lithium capacity trapped inside a (10,10) SWNT can be as high as $LiC_{2.6}$, and can be further improved after the lithium atoms trapped in the interstitial channels between SWNTs in bundles are taken into account. This implies that the bundles of SWNTs, especially large SWNTs, are ideal host materials with a high Li/C ratio, which can improve the energy density of Li-ion batteries.

## CONCLUSIONS

Although lithium can adsorb on both the interior and the exterior surfaces of SWNTs with the adsorption energy of around −2.4 eV, diffusion barriers are low with 0.046 eV for endohedral diffusion and 0.147 eV for exohedral diffusion in a (5,5) SWNT. Diffusion barriers slightly depend on the tube diameter. The energetically most economical diffusion pathway also depends on the chirality of the tube. Lithium atoms trapped inside SWNTs can form a one-dimensional linear chain and quasi-one-dimensional triangular nanotubes at low temperature.

## ACKNOWLEDGMENTS

We would like to thank James P. Lewis for the useful discussions in this on-going work. This work is supported by the National Natural Science Foundation of China under Grant Nos. 50402017, 10374059, and 90203013 and Foundation of Ministry of Education of China under Grant No. 20020422012.

*Author to whom correspondence should be addressed. Email address: zmw@sdu.edu.cn

[1] A. C. Dillon, K. M. Jones, T. A. Bekkedahl, C. H. Klang, D. S. Bethune, and M. J. Heben, Nature (London) **386**, 377 (1997).
[2] J. E. Fischer, Chem. Innovation **30**, 21 (2000).
[3] A. Thess, R. Lee, P. Nikdaev, H. Dai, P. Petit, J. Robert, C. Xu, Y. H. Lee, S. G. Kim, A. G. Rinzler, D. T. Colbert, G. E. Scuseria, D. Tomanek, J. E. Fischer, and R. E. Smalley, Science **273**, 483 (1996).
[4] M. M. Calbi, M. W. Cole, S. M. Gatica, M. J. Bojan, and G. Stan, Rev. Mod. Phys. **73**, 857 (2001), and references therein.
[5] B. W. Smith, M. Monthioux, and D. E. Luzzi, Nature (London) **396**, 323 (1998).
[6] M. Winter, J. O. Besenhard, M. E. Spahr, and P. Novak, Adv. Mater. (Weinheim, Ger.) **10**, 725 (1998).
[7] B. Gao, C. Bower, J. D. Lorentzen, L. Fleming, Y. Wu, and O. Zhou, Chem. Phys. Lett. **307**, 153 (1999).
[8] S. M. Lee, K. H. An, Y. H. Lee, G. Seifert, and T. Frauencheim, J. Am. Chem. Soc. **123**, 5059 (2001).
[9] Y. C. Ma, Y. Y. Xia, M. W. Zhao, R. J. Wang, and L. M. Mei, Phys. Rev. B **63**, 115422 (2001).
[10] S. M. Lee and Y. H. Lee, Appl. Phys. Lett. **76**, 2877 (2000).
[11] Y. C. Ma, Y. Y. Xia, M. W. Zhao, and M. J. Ying, Chem. Phys. Lett. **357**, 97 (2002).
[12] Y. Y. Xia, M. W. Zhao, Y. C. Ma, X. D. Liu, M. J. Ying, and L. M. Mei, Phys. Rev. B **67**, 115117 (2003).
[13] X. Zhao, Y. Ando, Yi. Liu, M. Jinno, and T. Suzuki, Phys. Rev. Lett. **90**, 187401 (2003).
[14] J. R. Dahn, Tao Zheng, Yinghu Liu, and J. S. Xue, Science **270**, 590 (1995); *Lithium Batteries: New Materials, Development, and Perspectives*, edited by G. Pisotia (Elsevier, New York, 1994).
[15] J. Zhao, A. Buldum, J. Han, and J. P. Liu, Phys. Rev. Lett. **85**, 1706 (2000).
[16] T. Kar, J. Pattanayak, and S. Scheiner, J. Phys. Chem. A **105**, 10397 (2001).
[17] V. Meunier, J. Kephart, C. Roland, and J. Bernholc, Phys. Rev. Lett. **88**, 075506 (2002).
[18] J. P. Lewis, K. R. Glaesemann, G. A. Voth, J. Fritsch, A. A. Demkov, J. Ortega, and O. F. Sankey, Phys. Rev. B **64**, 195103 (2001).
[19] M. Fuchs and M. Scheffler, Comput. Phys. Commun. **119**, 67 (1999).
[20] D. R. Hamann, Phys. Rev. B **40**, 2980 (1989).
[21] A. D. Becke, Phys. Rev. A **38**, 3098 (1988).
[22] C. Lee, W. Yang, and R. G. Parr, Phys. Rev. B **37**, 785 (1988).
[23] M. W. Zhao, Y. Y. Xia, J. P. Lewis, and L. M. Mei, J. Phys. Chem. B **108**, 9599 (2004).
[24] M. W. Zhao, Y. Y. Xia, J. P. Lewis, and R. Q. Zhang, J. Appl. Phys. **94**, 2398 (2003).
[25] M. W. Zhao, Y. Y. Xia, Y. C. Ma, M. J. Ying, X. D. Liu, and L. M. Mei., Phys. Rev. B **66** 155403 (2002).
[26] M. S. Anderson and C. A. Swenson, Phys. Rev. B **31**, 668 (1985).
[27] M. Khantha, N. A. Cordero, L. M. Molina, J. A. Alonso, and L. A. Girifalco, Phys. Rev. B **70**, 125422 (2004).
[28] M. J. Firsch *et al.*, computer code GAUSSIAN 98, Gaussian, Inc., Pittsburgh, PA, 1999.
[29] C. Wang, Q. M. Zhang, and J. Bernholc, Phys. Rev. Lett. **69**, 3789 (1992).
[30] D. Feller, D. A. Dixon, and J. B. Nicholas, J. Phys. Chem. A **104**, 11414 (2000).
[31] T. Tsuzuki, M. Yoshida, T. Uchimaru, and M. Mikami, J. Phys. Chem. A **105**, 769 (2001).
[32] J. C. Amicangelo and P. B. Armentrout, J. Phys. Chem. A **104**, 11420 (2000).
[33] Binding energies were calculated from the difference between the total energy of the Li-SWNT system and the energy of the corresponding isolated SWNT and lithium atom.
[34] Y. Kondo and K. Takayanagi, Science **289**, 606 (2000).
[35] Y. Oshima, A. Onga, and K. Takayanagi, Phys. Rev. Lett. **91**, 205503 (2003).